

Published in final edited form as:

Polyhedron. 2014 December 14; 84: 144–149. doi:10.1016/j.poly.2014.06.055.

Z-Selective Ruthenium Metathesis Catalysts: Comparison of Nitrate and Nitrite X-type Ligands

Melanie A. Pribisko, Tonia S. Ahmed, and Robert H. Grubbs*

Arnold and Mabel Beckman Laboratories of Chemical Synthesis, Division of Chemistry and Chemical Engineering, California Institute of Technology, Pasadena, CA 91125

Abstract

Two new Ru-based metathesis catalysts, **3** and **4**, have been synthesized for the purpose of comparing their catalytic properties to those of their *cis*-selective nitrate analogues, **1** and **2**. Although catalysts **3** and **4** exhibited slower initiation rates than **1** and **2**, they maintained high *cis*-selectivity in homodimerization and ring-opening metathesis polymerization reactions. Furthermore, the nitrite catalysts displayed higher *cis*-selectivity than **2** for ring-opening metathesis polymerizations, and **4** delivered higher yields of polymer.

1. Introduction

With increasing control of stereo and chemoselectivity, transition metal-catalyzed olefin metathesis is rapidly becoming ubiquitous and a preferred method for constructing carbon-carbon double bonds.¹ This process has gained widespread applicability in a variety of fields including organic synthesis, biochemistry, and materials science.² Transition metal catalysts that could selectively produce the kinetically favored *cis*-products remained elusive until the discovery of Group VI-based systems by Schrock and Hoveyda.³ *Cis*-selective Ru-based metathesis catalysts were developed soon thereafter, all containing a *N*-heterocyclic carbene (NHC) ligand.⁴ In 2011, we reported that *cis*-selectivity could be achieved with a ruthenium catalyst where the *N*-adamantyl substituent of an NHC has undergone C-H activation at Ru to impose unique geometrical constraints.⁵ During olefin metathesis, side-bound ruthenacycles are formed where the *N*-aryl NHC substituent dictates a *cis*-conformation of metallacycle substituents, resulting in production of the corresponding *Z*-olefin.^{6,7} Later *N*-adamantyl analogues with a bidentate nitrate ligand (catalysts **1** and **2**) displayed greater activity and stability.^{8,9} In 2013, the Jensen and Hoveyda groups independently reported *cis*-selective Ru-based metathesis catalysts with [H₂IMes₂] (H₂I=imidazolidinylidene, Mes=mesityl) NHC ligands, but different X-type ligands.^{10,11}

© 2014 Elsevier Ltd. All rights reserved.

*rhg@caltech.edu Phone: (626) 395-6003.

Publisher's Disclaimer: This is a PDF file of an unedited manuscript that has been accepted for publication. As a service to our customers we are providing this early version of the manuscript. The manuscript will undergo copyediting, typesetting, and review of the resulting proof before it is published in its final citable form. Please note that during the production process errors may be discovered which could affect the content, and all legal disclaimers that apply to the journal pertain.

In order to further probe the effect and role of the nitrate ligand in catalyst activity, stability, and selectivity of the Grubbs' systems, we herein report the synthesis of the nitrite analogues of these catalysts, **3** and **4**, and their reactivities for homodimerization and ring-opening metathesis polymerization reactions.¹²

2. Experimental

2.1 Materials and Methods

Unless otherwise stated, solvents and reagents were of reagent quality, obtained from commercial sources and used without further purification. Reactions involving catalysts **1-4** were carried out in a nitrogen-filled glovebox. Substrates for homodimerization were degassed by sparging with Ar(g) and liquids were filtered through a short plug of basic alumina prior to use. THF was purified by passage through solvent purification columns and degassed prior to use.

2.2 Preparation of catalyst **3**

In a N₂-filled glovebox, reaction of **5** (50 mg, 0.74 mmol) with 25 equivalents of AgNO₂ (285 mg, 1.8 mmol) in benzene yields **3** (33.6 mg, 0.5 mmol, 69 % yield) within one hour at room temperature. The reaction mixture was filtered to remove unreacted starting material and AgI, and the solvent was removed *in vacuo*. The solids were triturated with an ether/pentane solution to give catalyst **3** in a 63% yield. ¹H-NMR (600 MHz, C₆D₆) (†, ppm): 14.83 (s, 1H), 7.45 (d, 7.5 Hz 1H), 7.15 (m, 3H), 7.08 (dd, 7.5 Hz, 1 H), 7.02 (dd, 7.5 Hz, 1H), 6.85 (t, 7.5 Hz, 3H), 6.47 (d, 8.5 Hz, 1H), 4.54 (hept, 6.0 Hz, 1H), 3.77 (m, 2H), 3.51 (m, 1H), 3.34 (m, 1H), 3.24 (m, 1H), 3.08 (heptet, 6.5 Hz, 1H), 2.27 (s, 1H), 2.06 (s, 1H), 1.94 (t, 9.5 Hz, 2H), 1.80 (m, 3H), 1.64 (d, 6.5 Hz, 4H), 1.41 (m, 3H), 1.35 (d, 6.5 Hz, 3H), 1.29 (d, 7.0 Hz, 3H), 1.18 (d, 7.0 Hz, 3H), 1.15 (d, 7.0 Hz, 1H), 1.10 (d, 6.0 Hz, 2H), 1.08 (m, 2H), 0.88 (d, 6.0 Hz, 3H), 0.58 (d, 7.5 Hz, 1H). ¹³C-NMR (126 MHz, C₆D₆) (δ, ppm): 261.3, 212.1, 154.3, 147.4, 146.9, 142.8, 136.0, 128.5, 125.9, 124.0, 123.6, 123.1, 122.9, 122.9, 112.5, 74.4, 72.8, 67.4, 62.8, 54.0, 42.6, 41.2, 39.9, 37.6, 37.5, 37.3, 32.9, 30.5, 29.4, 28.3, 28.1, 28.1, 27.2, 26.4, 25.4, 25.4, 23.3, 22.4, 20.8, 20.1. HRMS (FAB⁺) calculated for C₃₅H₄₆O₃N₃Ru [(M+H)-H₂]⁺ 658.2583; found 658.2583.

2.3 Preparation of catalyst **4**

In a N₂-filled glovebox, reaction of **6** (50 mg, 0.79 mmol) with 7 equivalents of AgNO₂ (85 mg, 0.55 mmol) in benzene cleanly forms **4** (30.7 mg, 0.50 mmol, 63 % yield) over a reaction time of two hours at room temperature. The reaction mixture was filtered to remove unreacted starting material and AgI, and the solvent was removed *in vacuo*. The solids were triturated with ether for a 69% yield of catalyst **4**. ¹H-NMR (600 MHz, C₆D₆) (δ, ppm): 14.83 (s, 1H), 7.40 (d, 7.5 Hz 1H), 7.18 (t, 7.9 Hz, 1H), 6.84 (td, 7.4 Hz, 1H), 6.81 (s, 1H), 6.74 (s, 1H), 6.52 (d, 8.7 Hz, 1H), 4.59 (heptet, 6.45 Hz, 1H), 3.61 (s, 1H), 3.41 (heptet, 10.5 Hz, 1H), 3.23 (m, 3H), 2.45 (s, 3H), 2.32 (m, 1H), 2.23 (s, 3 H), 2.12 (t, 3.3 Hz, 3H), 2.09 (s, 3H), 2.00 (m, 2H), 1.91 (br d, 11.0 Hz, 1H), 1.79 (d, 12.0 Hz, 1H), 1.65 (m, 1), 1.48 (m, 2H), 1.39 (d, 6.4 Hz, 3H), 1.26 (m, 1H), 1.12 (m, 3H), 0.91 (d, 6.2 Hz, 7H), 0.61 (d, 12.2 Hz, 1H). ¹³C-NMR (400 MHz, C₆D₆) (δ, ppm): 259.5, 214.1, 154.3, 143.0, 137.4, 136.8, 136.3, 135.3, 129.4, 128.8, 125.8, 123.0, 122.9, 112.4, 74.3, 73.5, 67.4, 62.7, 51.3, 42.7,

41.3, 39.9, 37.6, 37.4, 37.1, 33.0, 30.6, 29.5, 25.4, 20.9, 20.6, 20.0, 18.3, 18.2. HRMS (FAB⁺) calculated for C₃₂H₄₀RuN₃O₃ [(M+H)-H₂]⁺ 616.2114; found 616.2119.

2.4 General procedure for homodimerizations

To an open 4 mL vial charged with a stir bar in a N₂-filled glovebox, 1.23 mmol of the olefin substrate and the appropriate volume of THF were added such that the total volume of the resulting solution was 225 μL. A solution of 1.23 μmol catalyst in 200 μL THF was added to the substrate and the reaction was stirred at 35 °C. At appropriate time points, 10 μL aliquots were taken and diluted with 0.70 mL chloroform-*d*₁ and analyzed using ¹H-NMR spectroscopy. The reactions were performed in duplicate and the numbers reported are the average of the two runs and the standard deviation observed.

2.5 General procedure for ROMP

In an 8 mL vial charged with a stir bar, 1 mL of 0.32 M stock solution of monomer was added under an argon atmosphere. A solution of 3.2 μmol catalyst in 275 μL THF was added and the reaction was stirred at room temperature. After 1 hour, the reaction was quenched with 50 μL ethyl vinyl ether. The reaction mixture was then precipitated into methanol. The polymer samples were collected on a fine frit, washed with several portions of methanol, and dried under vacuum.

2.6 General procedure for initiation rate determination

In a N₂-filled glovebox, a 4-mL vial was charged with catalyst (0.012 mmol) and dissolved with 100 μL C₆D₆. A portion of the stock solution (0.2 mL, 0.003 mmol) was added to a NMR tube and diluted with C₆D₆ (0.4 mL). The NMR tube was sealed with a septum cap and placed in the NMR spectrometer at 30 °C. Butyl vinyl ether (12 μL, 0.09 mmol) was added and the disappearance of the benzyldiene proton resonance was monitored by arraying the 'pad' function in VNMRj. All reactions showed clean first-order kinetics over a period of at least three half-lives. Spectra were baseline corrected and integrated using MestReNova.

2.7 Instrumentation

¹H-NMR spectra for homodimerization reactions were taken on Varian Inova 300 MHz and automated Varian Inova 500 MHz instruments. ¹H and ¹³C spectra for catalysts **3** and **4** were recorded on a Varian Inova 600 MHz instrument or an automated Varian Inova 500 MHz instrument (126 MHz for ¹³C). Initiation rate experiments were monitored using Varian Inova 500 MHz and Varian Inova 600 MHz instruments. High-resolution fast atom bombardment (FAB) mass spectrometry was performed at the California Institute of Technology Mass Spectrometry Facility. Molecular weights and polydispersity indexes of polymer samples were determined using multi-angle light scattering gel permeation chromatography, employing an Agilent 1200 UV-Vis detector and a Wyatt Technology miniDAWN TREOS light scattering detector, Viscostar viscometer, and OptilabRex refractive index detector. dn/dc values were determined by assuming 100% mass recovery of the sample to calculate molecular weights.

3. Results and Discussion

3.1 Synthesis

Previous studies demonstrated the nitrate X-type ligand on catalysts **1** and **2** exchanges to form the corresponding iodo complexes **5** and **6** (Scheme 1) upon exposure to excess NaI in THF.^{5a} It was found that these iodo complexes could be readily converted to the corresponding nitrito complexes, **3** and **4**, using excess AgNO₂ in benzene. Trituration with pentane/ether afforded the pure catalysts. The ¹H-NMR spectra of **3** and **4** were recorded in C₆D₆. Both complexes showed a characteristic singlet at 14.82 ppm, which can be assigned to the benzylidene proton and is slightly, but distinctly, shifted from the corresponding benzylidene singlets of the nitrate catalysts **1** and **2** (15.22 ppm). The corresponding carbon is observed at 261.3 ppm and 259.5 ppm for **3** and **4**, respectively, compared to 267.5 and 265.8 for the corresponding nitrate-ruthenium catalysts.

3.2 Homodimerizations

In order to elucidate differences in reactivity and *Z*-selectivity between the nitrate and nitrito catalysts, we subjected them to a standard set of substrates. The homodimerization of allylbenzene (**7**) is a good benchmark to determine the activity and stability of olefin metathesis catalysts. Since allylbenzene homodimerization occurs quickly with catalysts **1** and **2**, a low catalyst loading of 0.1 mol% was used to differentiate the new nitrite-containing catalysts from the highly active and *Z*-selective nitrate catalysts. Both catalysts **3** and **4** proved to be slower than the nitrate analogues, achieving 88% and 78% conversion, respectively, at 3 hours. In comparison, the reaction reached completion after approximately one hour with the nitrate catalysts. While slower, **3** and **4** are able to retain the high *Z*-selectivity seen in the nitrate catalysts. In the case of allylbenzene, catalyst **4** with the less bulky *N*-Mes substituent was found to achieve higher conversion over the course of the reaction compared to catalyst **3** with the more sterically hindered *N*-DIPP substituent. Such a difference is not observed with the nitrate catalysts.^{5a, 9a}

Conversion to the olefin migration product **9** is indicative of catalyst stability. At long time points when conversion of allyl benzene is complete or nearly complete, the ratio of **8** to **9** is comparable for all four of the catalysts (reported in Figure 2). This supports our observation that the new nitrite-containing catalysts are stable metathesis catalysts. We plan to further investigate isomerization and decomposition pathways of these catalysts, particularly since the nitrite-containing catalyst **4** appears to promote less formation of the olefin isomerization product than **1-3**.

Two more challenging homodimerization substrates, methyl undecenoate (**10**) and allyl acetate (**12**), were tested to further examine catalyst activity. At three hours, both nitrate catalysts achieved high conversion to the methyl undecenoate homodimer. In contrast, catalyst **4** had a modest conversion of 63% whereas **3** only achieved minimal conversion (13%). At twelve hours, **4** had a reasonable 81% conversion while **3** had reached 61% conversion. Here, there is a clear difference in conversion between the DIPP-NHC catalyst **3** and the Mes-NHC catalyst **4** that is not apparent with the nitrate catalysts **1** and **2**. This observable differentiation may be due more to an induction period before metathesis rather

than less active catalysts. For all four catalysts, the *Z*-selectivity remained above 95% at all conversions of methyl undecenoate. For allyl acetate, which is a challenging substrate for metathesis catalysts, we observed low conversions by catalysts **2**, **3** and **4** at three hours, but by five hours all catalysts were achieving comparable conversions, although the nitrito catalysts had slightly lower *Z*-selectivity. There is no clear difference in the rate of conversion for catalysts **2**, **3** and **4** for allyl acetate. In contrast, the DIPP-NHC nitrate catalyst **1** maintains a similar rate of conversion across the time period monitored. This difference in behavior will be investigated further through initiation rate studies.

With this obvious induction period where the nitrite-containing catalysts are initially slow but reach comparable overall conversion and similar *Z*-selectivity compared to catalysts **1** and **2**, we tested the initiation rate of catalyst reaction with butyl vinyl ether (BVE) substrate.¹³ Consistent with the results of the homodimerizations, the DIPP-NHC catalyst **3** was much slower than catalysts **1**, **2** and **4**. There is a clear trend that the DIPP-NHC catalysts have slower initiation when compared to the Mes-NHC catalysts and the nitrito-containing catalysts are slower to initiate than the nitrate catalysts. The order of magnitude difference seen for **3** is somewhat greater than expected, particularly as this is an extremely active and productive metathesis catalyst.

In previous initiation rate studies, electron donating ligands such as 2,2-dimethoxypropanoate (**16**) imparted greater initiation rates compared to a pivalate (**17**) X-ligand ($2.5 \times 10^{-3} \text{ s}^{-1}$ vs. $0.87 \times 10^{-3} \text{ s}^{-1}$, respectively).^{5a} Steric bulk also increased the rate; the much larger dicyclohexyl carboxylate group (**18**) has an initiation rate constant of $6.9 \times 10^{-3} \text{ s}^{-1}$ while the smaller methyl group (**19**) has a constant of $0.17 \times 10^{-3} \text{ s}^{-1}$.^{5a} Finally, the hapticity of this X-ligand plays a large role in the magnitude of initiation rate as monodentate X-ligands (**20**) required much longer times at elevated temperature (70 °C) to initiate. Recent theoretical studies predict the ability of nitrate and carboxylato ligands to convert between monodentate and bidentate conformations is critical for metallacycle stabilization.^{14,15} The inability of monodentate X-ligands to form multiple coordination modes may be the reason these catalysts often are slow to initiate and have negligible metathesis activity. The fact that **3** and **4** are metathesis active and stable supports a bidentate binding mode. In the case of the nitrite X-ligand, the Mes-NHC initiates at approximately half the rate constant of the nitrate analogue, and this trend is seen in the homodimerization reactivity. However, the DIPP-NHC nitrite catalyst **3** has an initiation rate constant an order of magnitude lower than its nitrate analogue, which is apparent in the low conversions at early time points. It is not a simple relationship between initiation rate and metathesis reactivity since catalyst **3** has comparable conversions at later time points for allylbenzene and allyl acetate.

When applied to ring-opening metathesis polymerization, the slow initiation rate of catalyst **3** is evident in the corresponding low yields, high PDI and, for **poly-23**, high M_n .^{1e} High M_n can be attributed to a high rate of propagation (k_p) relative to the rate of initiation (k_i) or incomplete catalyst initiation. This was observed for catalyst **2**, which has a slow initiation rate compared to faster initiating catalysts (**21**) not containing the Hoveyda chelate. The nitrite X-ligand catalysts resulted in greater *cis* content compared to catalyst **2**, although

higher PDIs were observed in the case of **poly-22**. In contrast to homodimerization reactions where **4** outperformed **2** in terms of *Z*-selectivity, in ROMP reactions **4** had comparable yields and higher *Z*-selectivity.^{1e} The generally poor initiation rates were evident in the resulting PDIs of the polymers. The tacticity and functional group tolerance of this catalyst will be investigated further, in addition to further testing of both **3** and **4** in homodimerizations and cross metathesis reactions.

4. Conclusion

In summary, salt metathesis of I-ruthenium complexes **5** and **6** with AgNO₂ results in stable, chelated *Z*-selective ruthenium olefin metathesis catalysts **3** and **4**. The nitrite-containing catalysts are slower initiating than the nitrito analogues and, therefore, have lower conversions at early time points in homodimerization and ring-opening metathesis polymerization. Both types of X-ligands result in exceptional *Z*-selectivity. This high *Z*-selectivity is retained at longer reaction times where, in many cases, catalysts **3** and **4** reach comparable conversions. Both **3** and **4** exhibit greater *cis*-selectivity in ring-opening metathesis polymerization than previously observed with **2**, and **4** gave higher yields.^{1e} Given that **3** and **4** have much slower initiation rates, the retention of reactivity and selectivity merits further investigation of these catalysts as well as examination of other X-type ligands.

Supplementary Material

Refer to Web version on PubMed Central for supplementary material.

Acknowledgments

This work was financially supported by the NIH (R01GM031332) and the NSF (CHE-1212767). NMR spectra were obtained on instruments funded by the NIH (RR027690). Materia is gratefully acknowledged for donation of metathesis catalysts **1** and **2**. We thank Naseem Torian for high-resolution mass spectrometry studies. The authors would like to thank Brendan Quigley for helpful discussions and assistance with NMR experiments and Dr. B. Keith Keitz for initial experiments.

References

1. a Scholl M, Ding S, Lee CW, Grubbs RH. *Org. Lett.* 1999; 1:953–956. [PubMed: 10823227] b Grubbs RH, Chang S. *Tetrahedron.* 1998; 54:4413–4450. c Schwab P, Grubbs RH, Ziller JW. *J. Am. Chem. Soc.* 1996; 118:100–110. d Grubbs RH, Miller SJ, Fu GC. *Acc. Chem. Res.* 1995; 28:446–452. e Keitz BK, Federov A, Grubbs RH. *J. Am. Chem. Soc.* 2012; 134:2040–2043. [PubMed: 22239675] f Quigley, B.L. Grubbs RH. *Chem. Sci.* 2013; 00:1–5. g Cannon JS, Grubbs RH. *Angew. Chem. Int. Ed.* 2013; 52:9001–9004.
2. a Herbert MB, Marx VM, Pederson RL, Grubbs RH. *Angew. Chem. Int. Ed.* 2013; 52:310–314. b Meek SJ, O'Brien RV, Llaveria J, Schrock RR, Hoveyda AH. *Nature.* 2011; 471:461–466. [PubMed: 21430774] c Yu M, Wang CB, Kyle AF, Jakubec P, Dixon DJ, Schrock RR, Hoveyda AH. *Nature.* 2011; 479:88–93. [PubMed: 22051677] d Marx VM, Herbert MB, Keitz BK, Grubbs RH. *J. Am. Chem. Soc.* 2013; 135:94–97. [PubMed: 23244210]
3. a Ibrahim I, Yu M, Schrock RR, Hoveyda AH. *J. Am. Chem. Soc.* 2009; 131:3844–3847. [PubMed: 19249833] b Flook MM, Jiang AJ, Schrock RR, Muller P, Hoveyda AH. *J. Am. Chem. Soc.* 2009; 131:7962–7966. [PubMed: 19462947] c Marinescu SC, Schrock RR, Muller P, Takase MK, Hoveyda AH. *Organometallics.* 2001; 30:1780–1782. [PubMed: 21686089] d Peryshkov DV, Schrock RR, Takase MK, Muller P, Hoveyda AH. *J. Am. Chem. Soc.* 2011; 133:20754–20757.

- [PubMed: 22107254] e Schrock RR. *Chem. Rev.* 2002; 102:145–179. [PubMed: 11782131] f Schrock RR, Hoveyda AH. *Angew. Chem. Int. Ed.* 2003; 42:4592–4633.
4. Endo K, Grubbs RH. *J. Am. Chem. Soc.* 2011; 133:8525–8527. [PubMed: 21563826]
 5. a Keitz BK, Endo K, Patel PR, Herbert MB, Grubbs RH. *J. Am. Chem. Soc.* 2012; 134:693–699. [PubMed: 22097946] b Keitz BK, Endo K, Herbert MB, Grubbs RH. *J. Am. Chem. Soc.* 2011; 133:9686–9688. [PubMed: 21649443]
 6. Liu P, Xu XF, Dong XF, Keitz BK, Herbert MB, Grubbs RH, Houk KN. *J. Am. Chem. Soc.* 2012; 134:1464–1467. [PubMed: 22229694]
 7. Jiang AJ, Zhao Y, Schrock RR, Hoveyda AH. *J. Am. Chem. Soc.* 2009; 131:16630–16634. [PubMed: 19919135]
 8. Previously, nitrate ligands have been shown to decrease activity for other Ru-based metathesis catalysts: M. Jovi M, Torker S, Chen P. *Organometallics.* 2011; 30:3971–3980. Buchmeiser MR, Ahmad I, Gurram V, Kumar PS. *Macromolecules.* 2011; 44:4098–4106.
 9. a Rosebrugh LE, Herbert MB, Marx VM, Keitz BK, Grubbs RH. *J. Am. Chem. Soc.* 2013; 135:1276–1279. [PubMed: 23317178] b Herbert MB, Lan Y, Keitz BK, Liu P, Endo K, Day MW, Houk KN, Grubbs RH. *J. Am. Chem. Soc.* 2012; 134:7861–7866. [PubMed: 22500642] c Torker S, Khan RKM, Hoveyda AH. *J. Am. Chem. Soc.* 2014; 136:3439–3455. [PubMed: 24533571]
 10. Occhipinti G, Hansen FR, Törnroos KW, Jensen VR. *J. Am. Chem. Soc.* 2013; 135:3331–3334. [PubMed: 23398276]
 11. Khan RKM, Torker S, Hoveyda AH. *J. Am. Chem. Soc.* 2013; 135:10258–10261. [PubMed: 23822154]
 12. Other nitrite-containing Ruthenium complexes: Michrowska A, Bujok R, Harutyunyan S, Sashuk V, Dolgonos G, Grela K. *J. Am. Chem. Soc.* 2004; 126:9318–9325. [PubMed: 15281822] Gordon CM, Feltham RD, Turner JJ. *J. Phys. Chem.* 1991; 95:2889–2894. Ru-NO₂. Ohtsu H, Oka N, Yamaguchi T. *Inorg. Chim. Acta.* 2012; 383:1–6.
 13. a Thiel V, Hendann M, Wannowius K–J, Plenio H. *J. Am. Chem. Soc.* 2012; 134:1104–1114. [PubMed: 22188483] b Torker S, Merki D, Chen P. *J. Am. Chem. Soc.* 2008; 130:4808–4814. [PubMed: 18341339] c Monsaert S, Vila AL, Drozdak R, Van Der Voort P, Verpoort F. *Chem. Soc. Rev.* 2009; 38:3360–3372. [PubMed: 20449055]
 14. Dang Y, Wang ZX, Wang X. *Organometallics.* 2012; 31:7222–7234.
 15. Dang Y, Wang ZX, Wang X. *Organometallics.* 2012; 31:8654–8657.

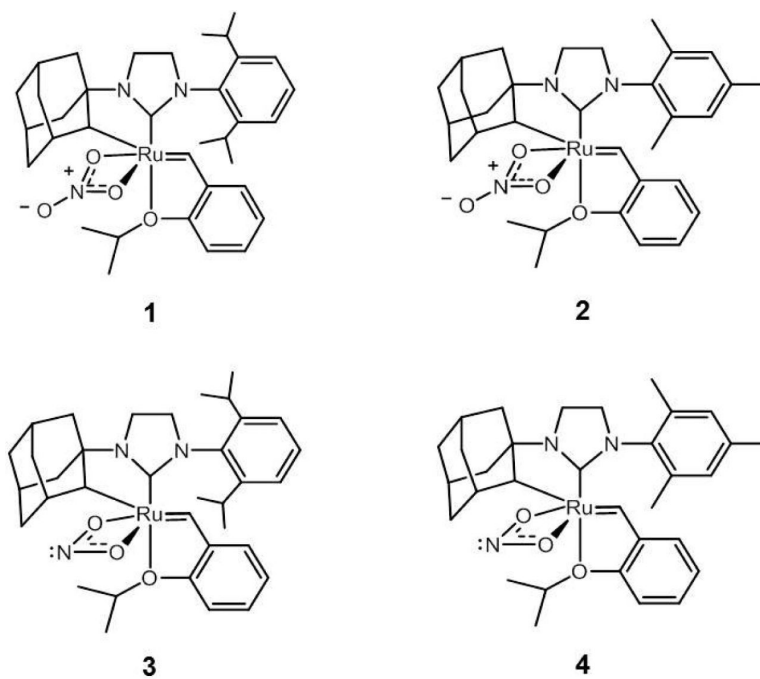
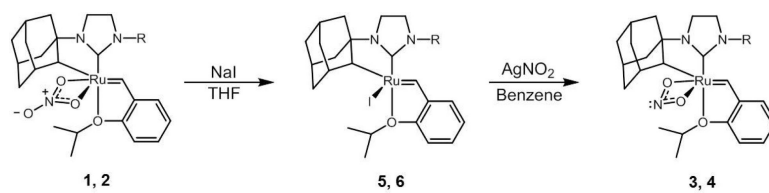
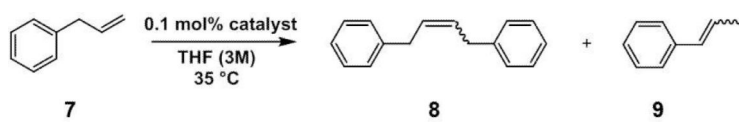


Figure 1. Catalysts **1-4** used for homodimerization and ring-opening metathesis polymerization reactions.



Scheme 1.
Preparation of Catalysts 3 and 4



Catalyst	Time (h)	Conv (%) ^a	Z-8 (%) ^a	8:9 ^b
1 (DIPP; NO ₃)	3	99	>95	22
2 (Mes; NO ₃)	3	100	>95	20
3 (DIPP; NO ₂)	3	78 (0.5)	>95	31
4 (Mes; NO ₂)	3	88	>95	16

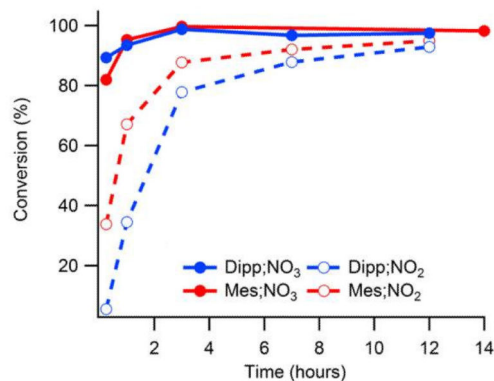
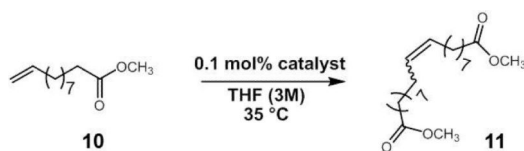


Figure 2.

Plots of percent conversion versus time for the homodimerization reaction of allylbenzene using 0.1 mol% **1-4** at 35 °C. ^aPercent conversion and Z-selectivity were determined using ¹H-NMR spectroscopy. ^bCross:Isomerization ratio was determined using ¹H-NMR spectroscopy at 12 hours.



Catalyst	Time (h)	Conv (%) ^a	Z (%) ^a
1 (DIPP; NO ₃)	3	94	>95
2 (Mes; NO ₃)	3	96	>95
3 (DIPP; NO ₂)	3	13	>95
4 (Mes; NO ₂)	3	63 (4)	>95

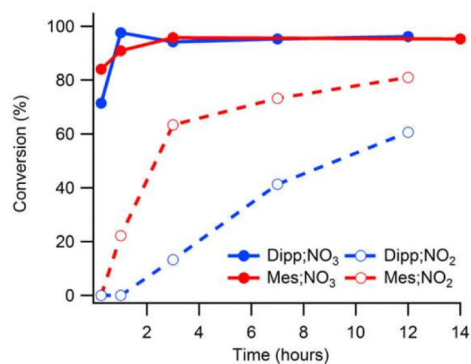
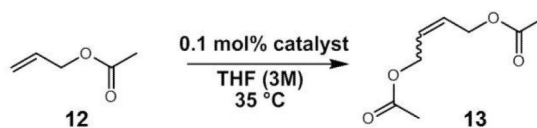


Figure 3. Plots of percent conversion versus time for the homodimerization reaction of methyl undecenoate using 0.1 mol% **1-4** at 35 °C. ^aPercent conversion and Z-selectivity were determined using ¹H-NMR spectroscopy.



Catalyst	Time (h)	Conv (%) ^a	Z (%) ^a
1 (DIPP; NO ₃)	3	43	>95
2 (Mes; NO ₃)	3	28	90
3 (DIPP; NO ₂)	3	18 (1)	94 (0.5)
4 (Mes; NO ₂)	3	13 (0.5)	86 (1)

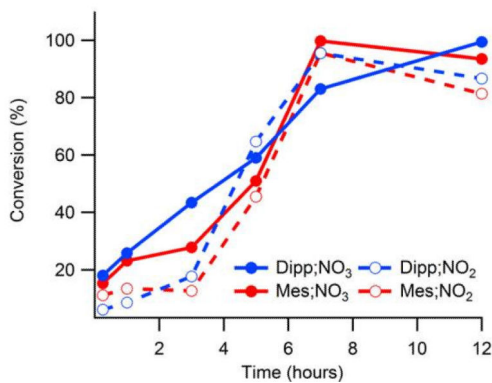


Figure 4. Plots of percent conversion versus time for the homodimerization reaction of allyl acetate using 0.1 mol% **1-4** at 35 °C. ^aPercent conversion and Z-selectivity were determined using ¹H-NMR spectroscopy.

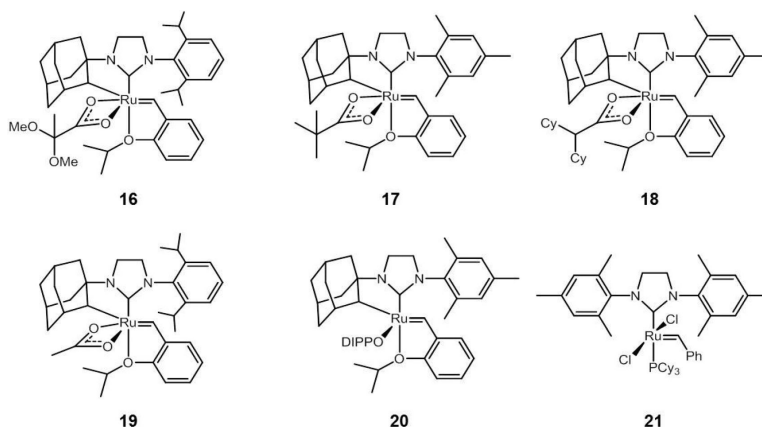
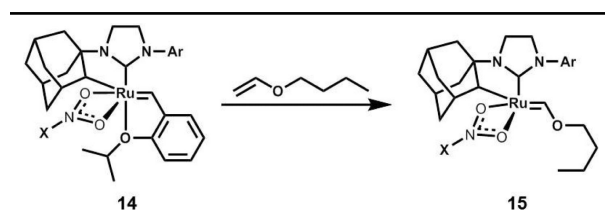


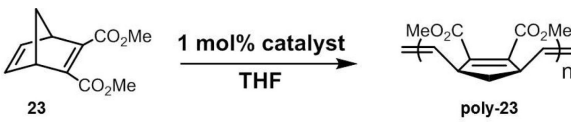
Figure 5.
Previously reported NHC-Ru metathesis catalysts.

Table 1

Initiation rates of the reaction of catalysts 1-4 with butyl vinyl ether as determined by $^1\text{H-NMR}$ spectroscopy.



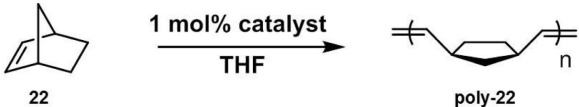
Catalyst	Temp (°C)	Initiation Rate Constant (10^{-4} s^{-1})
1 (DIPP; NO_3)	30	5.3
2 (Mes; NO_3)	30	8.4
3 (DIPP; NO_2)	30	0.4
4 (Mes; NO_2)	30	3.2

Table 2Ring-Opening Metathesis Polymerization of Monomer 22 with Catalysts 2-4.^{1e}


Catalyst	% cis ^a	Yield (%)	M_n (kDa)	PDI
2 (Mes; NO ₃)	88	94	347	1.87
3 (DIPP; NO ₂)	>95	15	24.9	2.44
4 (Mes; NO ₂)	94	>95	17.5	2.24

Table 3

Ring-Opening Metathesis Polymerization of Monomer 23 with Catalysts 2-4.



Catalyst	% cis ^a	Yield (%)	M_n (kDa)	PDI
2 (Mes; NO ₃)	86	91	— ^c	— ^c
3 (DIPP; NO ₂)	90	10	278	1.42
4 (Mes; NO ₂)	94	>95	57.2	1.23

^c M_n and PDI could not be determined due to insolubility in THF.^{1e}